The Journal of Chemical Physics

RESEARCH ARTICLE | APRIL 08 2021

Formation of covalently bound $C_4H_4^+$ upon electron-impact ionization of acetylene dimer

Yingying Wang; Enliang Wang ; Jiaqi Zhou ; Alexander Dorn ; Xueguang Ren

J. Chem. Phys. 154, 144301 (2021)
https://doi.org/10.1063/5.0045531

The Journal of Chemical Physics ARTICLE scitation.org/journal/jcp

Formation of covalently bound $C_4H_4^+$ upon electron-impact ionization of acetylene dimer

Cite as: J. Chem. Phys. 154, 144301 (2021); doi: 10.1063/5.0045531
Submitted: 27 January 2021 • Accepted: 24 March 2021 •
Published Online: 8 April 2021

Yingying Wang,[1] Enliang Wang,[2,3,a)] Jiaqi Zhou,[1,2] Alexander Dorn,[2] and Xueguang Ren[1,2,b)]

AFFILIATIONS

[1]MOE Key Laboratory for Nonequilibrium Synthesis and Modulation of Condensed Matter, School of Physics, Xi'an Jiaotong University, Xi'an 710049, China
[2]Max-Planck-Institut für Kernphysik, 69117 Heidelberg, Germany
[3]J. R. Macdonald Laboratory, Department of Physics, Kansas State University, Manhattan, Kansas 66506, USA

[a)]**Electronic mail:** enliang@phys.ksu.edu
[b)]**Author to whom correspondence should be addressed:** renxueguang@xjtu.edu.cn

ABSTRACT

We investigate the formation mechanisms of covalently bound $C_4H_4^+$ cations from direct ionization of hydrogen bonded dimers of acetylene molecules through fragment ion and electron coincident momentum spectroscopy and quantum chemistry calculations. The measurements of momenta and energies of two outgoing electrons and one ion in triple-coincidence allow us to assign the ionization channels associated with different ionic fragments. The measured binding energy spectra show that the formation of $C_4H_4^+$ can be attributed to the ionization of the outermost $1\pi_u$ orbital of acetylene. The kinetic energy distributions of the ionic fragments indicate that the $C_4H_4^+$ ions originate from direct ionization of acetylene dimers while ions resulting from the fragmentation of larger clusters would obtain significantly larger momenta. The formation of $C_4H_4^+$ through the evaporation mechanism in larger clusters is not identified in the present experiments. The calculated potential energy curves show a potential well for the electronic ground state of $(C_2H_2)_2^+$, supporting that the ionization of $(C_2H_2)_2$ dimers can form stable $C_2H_2 \cdot C_2H_2^+(1\pi_u^{-1})$ cations. Further transition state analysis and *ab initio* molecular dynamics simulations reveal a detailed picture of the formation dynamics. After ionization of $(C_2H_2)_2$, the system undergoes a significant rearrangement of the structure involving, in particular, C–C bond formation and hydrogen migrations, leading to different $C_4H_4^+$ isomers.

I. INTRODUCTION

The growth of carbonaceous molecules forming longer chains or polycyclic aromatic hydrocarbons (PAHs) is of great relevance to a wide variety of fields ranging from astrochemistry to material science.[1,2] The hydrocarbon molecules, such as acetylene, cyclobutadiene, benzene, and larger PAHs, have been found in interstellar clouds and medium, solar nebulae, and in envelopes expelled by evolved stars.[3–10] These species are believed to undergo complex dissociation and synthesis reactions in the interstellar medium (ISM), particularly in dense and cold molecular clouds, and also at the higher densities and temperatures found in planetary atmospheres.[11,12] Acetylene molecule (C_2H_2) serves as the basic precursor of the carbon-containing species. Clustering of acetylene molecules under ionizing radiation can play an important role in the formation of unsaturated hydrocarbons, such as benzene and larger PAHs, observed in the ISM.[3,4,13]

The underlying mechanisms for the formation of hydrocarbons have been probed using mass spectrometry and various spectroscopic techniques, as well as quantum chemistry calculations.[14–18] Nevertheless, the growth mechanisms of such complex systems remain incompletely understood even for the production of simple ions such as $C_4H_4^+$. Here, the structure of the covalently bound $C_4H_4^+$ "core ion" could play an important role in the cluster-mediated ion chemistry.[5,16] Ono and Ng reported the first observation of $C_4H_4^+$ from direct photoionization of acetylene dimers with

an onset energy of 10.4 eV (1188 Å), indicating that the ionization of the outermost $1\pi_u$ orbital of $(C_2H_2)_2$ dimers leads to the formation of $C_4H_4^+$.[14]

On the other hand, several recent studies suggested that the stable $C_4H_4^+$ cations are mainly formed through the fragmentation of larger clusters where the evaporation of neutral species provides the opportunity to reduce the internal energy and to finally form the stable ions.[5,16,17,19–21] It is also noted that the ionized acetylene trimer can form a very stable structure similar to that of the benzene cation.[15,20] The formation of larger hydrocarbons from acetylene cluster isomerization is usually accompanied by proton transfer or hydrogen migration (HM in brief), which lowers the potential energy by transforming it into internal energy that accelerates the reaction.[22–25] Recent studies showed that the HM can stabilize the repulsive potential energy surface (PES) of the dication before the Coulomb explosion.[24,26] Previous works obtained four isomers of the $C_4H_4^+$ ions, which are 1-buten-3-yne, methylenecyclopropene, 1,2,3-butatriene, and cyclobutadiene. This indicates the existence of HM and the rearrangement of the structure during the formation of $C_4H_4^+$ (see, e.g., Refs. 5, 19, 27, and 28).

In this work, we study the formation mechanisms of $C_4H_4^+$ upon electron-impact ionization (E_0 = 90 eV) of weakly bound acetylene dimers $(C_2H_2)_2$. The understanding of processes initiated by low energy electrons in matter is practically important,[29–31] since secondary electrons (<100 eV) are produced abundantly by high-energy ionizing radiation and are responsible for most of the radiation effects in media.[32–34] Employing coincident ion and electron momentum spectroscopy complemented with theoretical calculations, we find that the ionization of the outermost $1\pi_u$ acetylene orbital initiates a significant rearrangement of the dimer structure, leading to the formation of covalently bonded $C_4H_4^+$ cations.

Experimentally, the momentum vectors and, consequently, the kinetic energies for all three charged particles are determined: the singly charged ion, the scattered electron, and the ionized electron. We deduce the correlation of the ionic fragment species with the ionized electron's binding energy (BE) from which the ionized molecular orbital is identified. E_b represents the vertical transition energy between the electronic ground state and an ionized state of the molecule. The measured BE spectrum shows that $C_4H_4^+$ is formed by the removal of an electron from the highest occupied molecular orbital (HOMO) of acetylene. To reveal the formation dynamics, we performed quantum chemistry calculation of the potential energy surfaces, transition state (TS) analysis, and *ab initio* molecular dynamics (AIMD) simulations. Our study thus provides insight into the details of covalent bond formation, which is of great relevance for understanding the growth of hydrocarbons in the ISM.

II. EXPERIMENTAL AND THEORETICAL METHODS

The experiments were carried out using a reaction microscope, which was particularly designed for electron-impact experiments. Details of the experimental setup can be found elsewhere,[25,35–37] and only a brief introduction is given here. The pulsed electron beam was produced by a photoemission electron gun, which consists of a tantalum photocathode and electrostatic focusing lens. The wavelength, repetition rate, and pulse width of the laser are 266 nm, 40 kHz, and 0.5 ns, respectively. The acetylene dimer was generated by expanding the pure acetylene gas (2.5 bars) through a 30 μm nozzle into a vacuum chamber and collimated by two skimmers with aperture diameters of 200 μm, which are located about 3 mm and 2 cm downstream from the nozzle. The fraction ratio of monomers to dimers was estimated to be 1:0.015, and the contribution of larger clusters is below 10% of the dimers.

The electrons and ions produced in the collision volume were accelerated by a homogeneous electric and magnetic field onto the time- and position-sensitive detectors. Thus, a time-of-flight mass spectrum of the ionic fragments is obtained. Additionally, the momentum vectors of the outgoing charged particles were reconstructed from the measured times-of-flight and positions of the particles hitting the detectors. We detected the momenta of two outgoing electrons and one cation in triple-coincidence; thus, this constitutes a kinematically complete experiment for single ionization of acetylene monomers and dimers. The projectile energy E_0 and the measured energies E_1 and E_2 of the scattered and ejected electrons, respectively, are used to deduce the BE E_b of the ionized molecular orbitals: $E_b = E_0 - (E_1 + E_2)$. The BE resolution is ΔE_b = 3.0 eV, full width at half-maximum (FWHM), and it is calibrated using argon as a reference. Such BE spectra can be obtained for each resolved line in the ion TOF spectrum and, therefore, for each individual ionic fragment channel.[36] The comparison with published high-resolution photoelectron measurements for acetylene enables the identification of the ionized molecular orbitals.[38]

The quantum chemistry calculation was performed by the Gaussian package.[39] The AIMD simulation was carried out using the atom-centered density matrix propagation (ADMP) method[40–42] with a time range and a step size of 1000 and 0.5 fs, respectively. Here, the ωB97XD density-functional theory is used together with the cc-pVTZ basis set. To obtain a well adiabatic dynamics, the keyword "FULLSCF" is used, which produces an equivalent result as the Born–Oppenheimer molecular dynamics (BOMD). The initial condition of the simulation is obtained by a quantum harmonic oscillator distribution, which simulates the zero-point vibration of the neutral acetylene dimer. We assume a vertical transition from the neutral to the singly ionized ground state of the dimer, i.e., the removal of an electron from the outermost $1\pi_u$ orbital of acetylene.[19,36] To determine the crucial geometries during the dynamical evolution, the potential energy surface of the reaction coordinate is analyzed using the same quantum chemistry method. The obtained TSs and the corresponding reaction paths were confirmed by the intrinsic reaction coordinate (IRC) calculation.

III. RESULTS AND DISCUSSION

The measured ion time-of-flight spectrum is presented in Fig. 1(a). This spectrum shows several peaks 1–7, which can be assigned to C_2^+, C_2H^+, $C_2H_2^+$, ($^{13}C_2H_2^+$ and $C_2H_3^+$), $C_4H_3^+$, $C_4H_4^+$, and $C_4H_5^+$ cations, respectively. In the following, we focus mainly on the ionization channels related to the $C_2H_2^+$ and $C_4H_4^+$ cations.

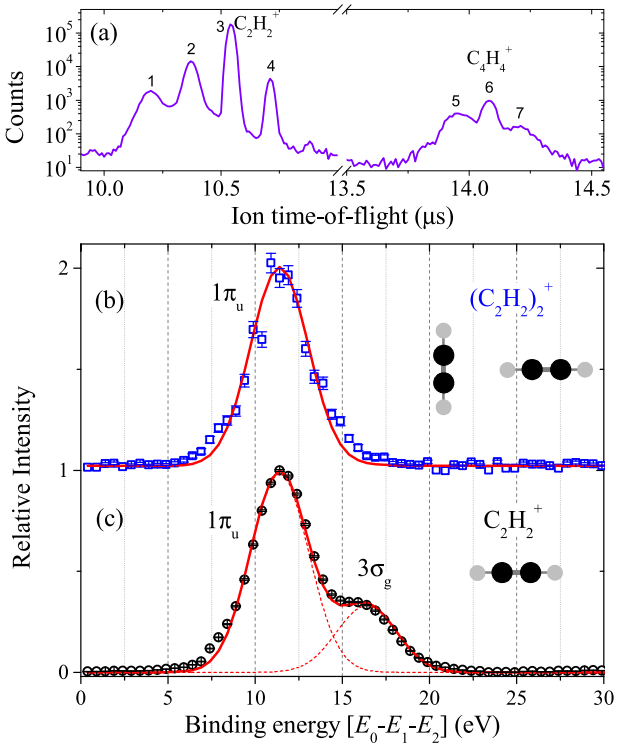

FIG. 1. (a) Experimental ion time-of-flight spectrum. The peaks correspond to (1) C_2^+, (2) C_2H^+, (3) $C_2H_2^+$, (4) $^{13}C_2H_2^+$ and $C_2H_3^+$, (5) $C_4H_3^+$, (6) $C_4H_4^+$, and (7) $C_4H_5^+$. (b) and (c) Measured binding energy spectra of dimers and monomers for the formation of (b) $C_4H_4^+$ and (c) $C_2H_2^+$ cations, respectively. The spectra are normalized to unity at the peak maximum, and (b) is offset for better visibility.

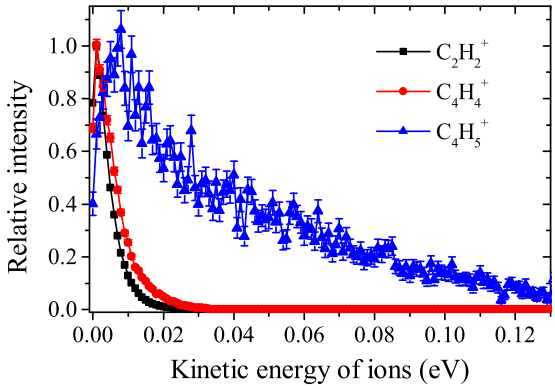

FIG. 2. Measured kinetic energy distributions of $C_2H_2^+$, $C_4H_4^+$, and $C_4H_5^+$ cations. The spectra are normalized to unity at the peak maximum.

The ground state electronic configuration of acetylene can be expressed as $(1\sigma_g)^2(1\sigma_u)^2(2\sigma_g)^2(2\sigma_u)^2(3\sigma_g)^2(1\pi_u)^4$.[43] The experimental BE spectrum in coincidence with the $C_2H_2^+$ parent ion is shown in Fig. 1(c). The peaks in this spectrum can be assigned to the production of vacancies, in particular, molecular orbitals. By fitting Gaussians to the data, two BE peaks at 11.4 and 16.7 eV are identified with a ratio of 1:0.33, which correspond to the ionization of the $(1\pi_u)$ and $(3\sigma_g)$ orbitals of acetylene, respectively.[43–45] On the contrary, for the $C_4H_4^+$ cations, shown in Fig. 1(b), we obtain a single peak structure of the BE located at about 11.4 eV. This means that the production of $C_4H_4^+$ is attributed to the ionization of $1\pi_u$ HOMO orbital of acetylene only.[14] The absence of other inner-valence shell ionization channels for $C_4H_4^+$ implies that the potential energy surfaces of these ionic states are repulsive or the internal energy is sufficiently high to induce the dissociation of the system. As will be discussed below, here we find that the latter is the case.

In the following, we provide evidence that $C_4H_4^+$ is formed by the direct ionization of acetylene dimers and not from the dissociation of larger clusters. If a non-dissociative ion is produced, its kinetic energy originates from the recoil momentum generated by electron-impact and the finite thermal energy of the target, both of which are very small leading to a sharp recoil-ion energy distribution with a peak value of a few meV. The measured kinetic energy (KE) distributions for ionic fragments are presented in Fig. 2, which show sharp distributions for the $C_2H_2^+$ and $C_4H_4^+$ cations with mean energies of about 4.7 and 6.3 meV, respectively. This indicates that these ions are formed through the direct ionization of acetylene monomers and dimers, respectively. The small difference in the spectral width of these two ions can be attributed to a slightly worse momentum resolution of the spectrometer for more heavy ion species. For comparison, we also plot the KE distribution of $C_4H_5^+$ ions in Fig. 2, which can result from dissociation processes such as $(C_2H_2)_3^+ \rightarrow C_4H_5^+ + C_2H$. The $C_4H_5^+$ ion resulting from the fragmentation of clusters obtain significantly larger momenta, i.e., higher KE (mean energy ~ 43.5 meV), due to the dissociative nature of the process.[46]

In order to reveal the underlying dynamics for the formation of $C_4H_4^+$, we perform AIMD simulations and TSs analysis. There exist several minima on the potential energy surface of the neutral acetylene dimer.[47–49] The two lowest ones are the T-shaped and slipped parallel structures in which the T-shaped structure is the more stable one.[17] In this work, we considered an optimized T-shaped dimer corresponding to the global energy-minimum geometry [shown in the inset of Fig. 1(b)]. In the T-shaped arrangement, the positively charged hydrogen points to the π electron cloud of the other acetylene, i.e., the CH-π interaction governs the structure of the dimer.[15,17,19] In contrast, the acetylene dimer cation $(C_2H_2)_2^+$ with the T-shaped structure is not an energy minimum on the ionic potential energy surface. Therefore, the T-shaped structure would rapidly rearrange to a more stable structure toward the covalently bonded molecular ion.[27]

The simulated trajectories for the $C_4H_4^+$ formation are shown in the left column of Fig. 3, which present the center-of-mass distances between the two acetylene monomers as a function of time. In our simulations, we found three possible reaction pathways for the formation of stable $C_4H_4^+$. Among 129 trajectories, 45, 74, and 10 trajectories ended up with cyclobutadiene (CB), methylenecyclopropene (MCP), and 1,2,3-butatriene (BT) ions, respectively. The vertical ionization of the acetylene dimer leads to a significant rearrangement of the $(C_2H_2)_2^+$ dimer ion structure. The two acetylene

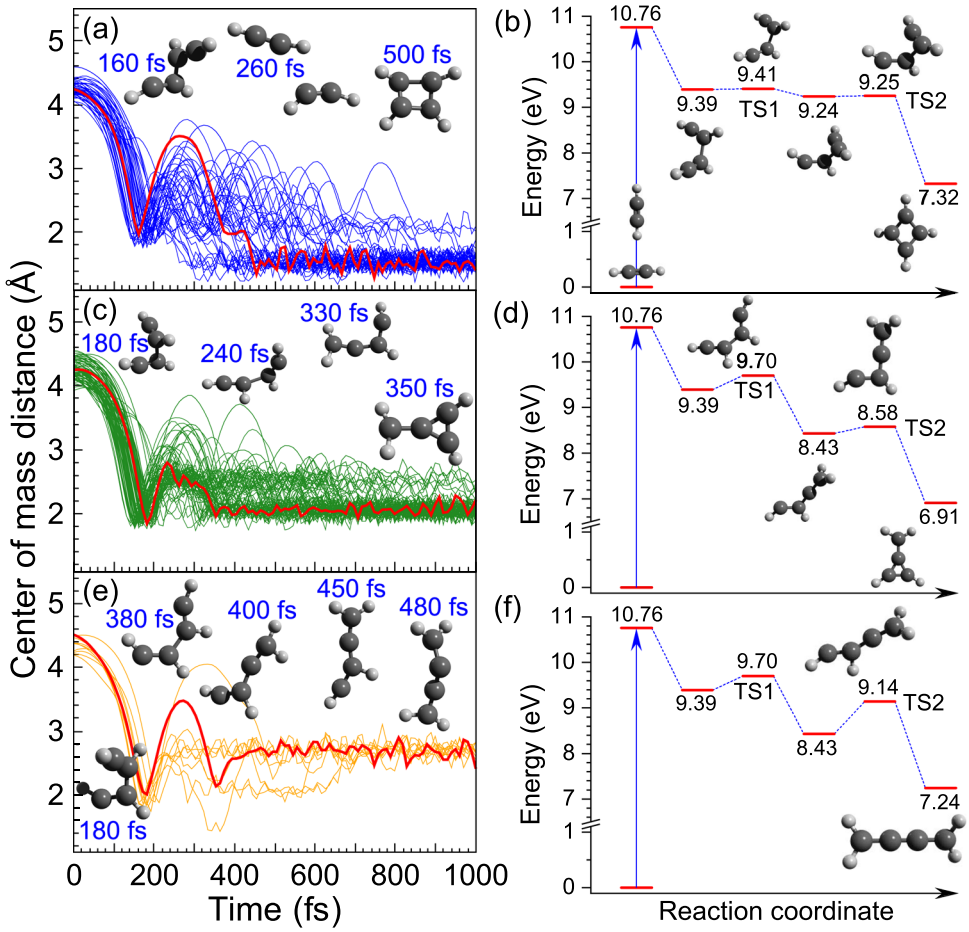

FIG. 3. *Ab initio* molecular dynamics simulations and potential energy surfaces for $C_4H_4^+$ formation. (a), (c), and (e) present the center-of-mass distance between the two acetylene monomers as a function of time. One typical trajectory corresponding to the red curve is shown in each panel. (b), (d), and (f) exhibit the relative potential energy as a function of the reaction coordinate for the transition states. The panels in the first, second, and third rows correspond to the formation of CB, MCP, and BT ions. The energies in panels (b), (d), and (f) are corrected by the zero-point energies (ZPEs).

monomers first come close to each other to form the covalent bond at about 160/180 fs. This bond formation process is consistent with the results described in Ref. 27. Driven by the internal energy, the two monomers start to rotate relative to the formed C–C bond. The dynamical evolution provides a possibility for the internal energy redistribution among other degrees of freedom, e.g., the vibrational motions. As shown in Fig. 3(a), the second C–C bond, i.e., a closed ring structure, is formed after about 400 fs.

The internal energy redistribution can also cause HM from one carbon to another. This can be seen in Figs. 3(c) and 3(e) where one and two hydrogen migrations lead to the formation of MCP and BT structures, respectively. Here, MCP is found to be the more stable isomer due to its lower potential energy of the final-state ion, as shown in Fig. 3(d). The formation of MCP is the predominant channel in our AIMD simulations since 57% of the simulated trajectories ended up with the MCP structure, while CB as the less stable isomer was considered to be dominant in previous studies,[5,16] which may be considered as an open issue.

The crucial points during the dynamical evolution are analyzed using the TSs, shown in the right column of Fig. 3, and the reaction paths are confirmed by the IRC calculation. Upon vertical ionization, the cation in the T-shaped structure is not the local minimum on the PES. Thereby, the system relaxes on the cationic PES along the energy minimum path. During the structure rearrangement, the first local minimum is reached at 9.39 eV, which corresponds to the formation of the first covalent bond during the dynamical evolution in the left column of Fig. 3. Afterward, there are two possible TSs (9.41 and 9.70 eV) for the reaction pathways. The first pathway undergoes a ring closing vibration as shown by TS1 (9.41 eV) in Fig. 3(b), and the second one corresponds to HM from one central carbon to the nearest terminal carbon as shown by TS1 (9.70 eV) in Figs. 3(d) and 3(f). For the pathway in Fig. 3(b), further relative rotation of the two acetylene encounters another TS2 (9.25 eV) and finally leads to the CB ion. This reaction path is in line with the previous studies.[16,19,27]

For the second and third reaction pathways, the forward reaction coordinate of the first HM is identical. After reaching the second local minimum (8.43 eV) on the potential energy surface, the reaction pathways are further separated into two channels. The lower energy TS2 (8.58 eV) corresponding to the tri-carbon ring closing can lead to the formation of the MCP ion, as shown in Fig. 3(d). The other pathway through a higher energy TS2 (9.14), corresponding to

TABLE I. Comparison of energetic calculations between different methods. TS1 and TS2 represent the transient states mentioned in this work. ΔE is the energy of the final-state ion. All energies including TS1 and TS2 are relative to the CB final-state. E represents the excess energy of the system in the reaction path. The unit of all numbers is eV.

	ROHF/6-31G*[a]			UQCISD/6-31G*[a]			UCCSD(T)/cc-pVTZ[a]			ωB97XD/cc-pVTZ[b]		
Ion	CB	MCP	BT	CB	MCP	BT	CB	MCP	BT	CB	MCP	BT
TS1	[c]	1.88	1.88	1.92	2.21	2.21	1.92	2.30	2.30	2.09	2.38	2.38
TS2	1.81	1.37	2.21	1.81	1.21	1.88	1.82	1.25	1.82	1.93	1.26	1.82
ΔE	0	−0.81	0.15	0	−0.42	−0.05	0	−0.30	0.01	0	−0.41	−0.08
E	3.24	4.05	3.09	3.40	3.82	3.45	3.42	3.73	3.42	3.44	3.85	3.52

[a]From Ref. 27. MCP: TS1 and TS2 represent LC2 and TS3 in Ref. 27, respectively. BT: TS1 and TS2 represent LC2 and TS4 in Ref. 27, respectively. The ZPEs relative to that of rectangular CB are added to the energies in Ref. 27.
[b]Our experimental results.
[c]Could not be located in the references.

the second HM from the middle carbon to its neighboring terminal carbon, forms the BT ion as shown in Fig. 3(f). It is noted that the 1-buten-3-yne ion[5,14,28] is not observed in our simulation. This can be due to the higher energy barrier to be overcome for this reaction pathway.[27] In Table I, the calculated potential energies of different states are compared with the literature values.[27] This shows that the present calculation (ωB97XD/cc-pVTZ) is in reasonable agreement with the energy levels calculated using UCCSD(T)/cc-pVTZ and UQCISD/6-31G* methods where the energy deviations are smaller than 0.2 eV, while the deviations of the ROHF/6-31G* method can be as large as 0.5 eV.

Finally, we consider the stability of the cationic acetylene dimer $(C_2H_2)_2^+$ by analyzing the relative potential energy curves (PECs) of $(C_2H_2)_2$ and $(C_2H_2)_2^+$ along the intermolecular distance (R) calculated using MP2/aug-cc-pVTZ method. It is shown in Fig. 4 that the dissociation limit is higher than the vertical ionization point (see the orange arrow). The calculated PECs in Fig. 4 show a potential well for the electronic ground state of $(C_2H_2)_2^+$, indicating that ionization of the HOMO in $(C_2H_2)_2$ dimers can create stable $C_2H_2{\cdot}C_2H_2^+(1\pi_u^{-1})$ cations. Our further AIMD simulations (up to 10 ps), shown in Fig. 5, reveal that the internal energies of the $C_4H_4^+$ cation are mostly redistributed to the vibrational motions of the system. It is found that the $C_4H_4^+$ cation is stable within the time range considered for high vibrational energies (1.5–3.5 eV) [see Figs. 5(a)–5(d)], i.e., the evaporation of neutral C_2H_2 from $C_4H_4^+$ is unlikely

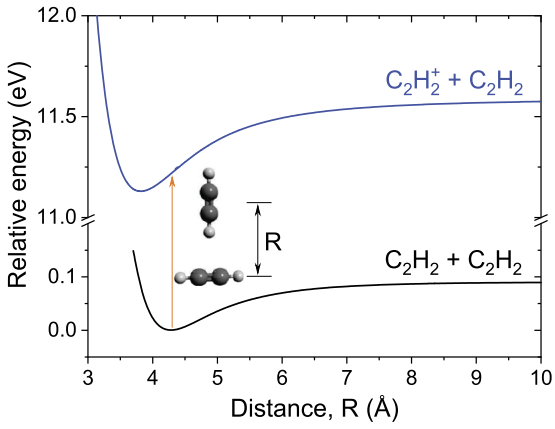

FIG. 4. Potential energy curves of neutral and cationic acetylene dimers as a function of center-of-mass distance calculated by the rigid PES scan using the MP2/aug-cc-pVTZ method.

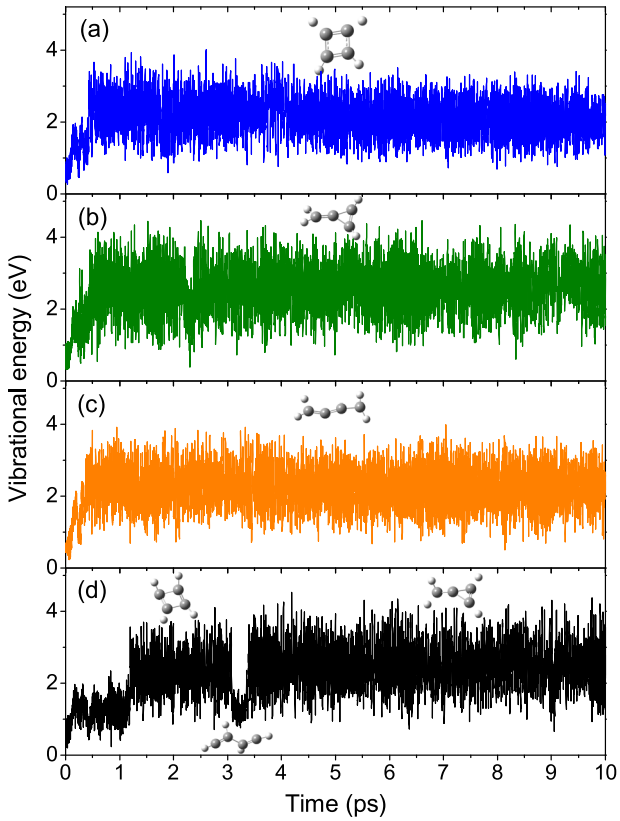

FIG. 5. Calculated internal vibrational energy as a function of evolution time up to 10 ps for the formation of the covalent bond $C_4H_4^+$ cations in the forms of CB (a), MCP (b), and BT (c). The cation structures can also convert, e.g., from CB to MCP forms in (d).

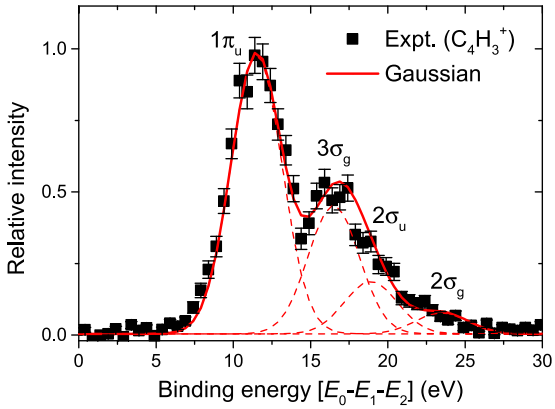

FIG. 6. Measured binding energy spectrum for the formation of $C_4H_3^+$.

to occur based on our calculations. As will be discussed below, we observe a decay channel for emission of neutral hydrogen, which seems to be the preferred decay channel for longer times or for higher internal energies.

Interestingly, we also found that during the dynamical evolution, the $C_4H_4^+$ cations can convert from the CB to the MCP form via a low-energy covalent bond structure as shown in Fig. 5(d). This indicates a rather high stability of the covalent bond formed between two C_2H_2 monomers. As the chemical reactivity in ion–molecule reactions sensitively depends on the internal energy of the ionic species, the high vibrational energy stored in $C_4H_4^+$ can support its high reactivity as "core ion" for formation processes of larger hydrocarbons in the ISM.[5,16]

Moreover, in Fig. 6, we present the measured BE spectrum for the formation of $C_4H_3^+$ ions, i.e., for emission of neutral hydrogen. This spectrum shows four peaks located at BE = 11.5, 16.7, 18.9, and 23.5 eV, corresponding to the ionization of $1\pi_u$, $3\sigma_g$, $2\sigma_u$, and $2\sigma_g$ orbitals, respectively. The obtained ratios are 1:0.46:0.19:0.075. The observation of the $1\pi_u$ ionization channel for $C_4H_3^+$ shows that, on a longer time scale, the high internal energy of the $C_4H_4^+$ ion may lead to emission of neutral hydrogen for a fraction of the ions. Significantly higher internal energy is available for ionization of the more strongly bound orbitals $3\sigma_g$, $2\sigma_u$, and $2\sigma_g$. The resulting acetylene dimer ion is unstable, and H emission is observed. For this $C_4H_3^+$ channel, a contribution from the ionization of larger clusters cannot be fully excluded.

IV. SUMMARY

We have reported a combined experimental and theoretical study on the formation mechanisms of $C_4H_4^+$ cations upon electron-impact ionization of weakly bound acetylene dimers $(C_2H_2)_2$. The experiments were performed using a fragment ion and electron coincident momentum imaging technique (reaction microscope) in which the momenta and energies of all three final-state particles (two electrons plus one ion) are detected in triple-coincidence. The ionization channels leading to the production of $C_2H_2^+$ and $C_4H_4^+$ cations from acetylene monomers and dimers, respectively, have been identified through the measurement of binding energy spectra. It is observed that the ionization of $1\pi_u$ and $3\sigma_g$ orbitals of the acetylene molecule can lead to the stable $C_2H_2^+$ ion, while the $C_4H_4^+$ cation is formed only by the ionization of the outermost $1\pi_u$ orbital. The measured kinetic energy distributions of different ions indicate that the $C_4H_4^+$ ions are attributed to the direct ionization of $(C_2H_2)_2$ dimers, while the fragmentation of larger clusters $(C_2H_2)_n$, $n \geq 3$, would result in significantly larger momenta that are not observed in the present experiments.

The calculated potential energy curves show a potential well for the electronic ground state of $(C_2H_2)_2^+$, supporting that the direct ionization of $(C_2H_2)_2$ dimers can create stable $C_2H_2{\cdot}C_2H_2^+(1\pi_u^{-1})$ cations. Further transition state analysis and molecular dynamics simulations reveal a detailed picture for the formation dynamics of $C_4H_4^+$. After the ionization of the acetylene dimer, the system undergoes a significant rearrangement. In particular, C–C bond formation and hydrogen migration lead to different isomers of the stable $C_4H_4^+$ cations that are methylenecyclopropene, cyclobutadiene, and 1,2,3-butatriene ions. We notice that for dimers once a covalent bond is formed between the two monomers, there is no further weakly bound moiety that can take away the internal energy. The internal energy of dimer ions is mostly distributed into the vibrational modes of the system, which can maintain the stability of $C_4H_4^+$ cations. These results provide new insight on the cluster-mediated ion chemistry in the interstellar medium. Future time-resolved studies using ultrashort pulses, e.g., from free electron lasers,[50,51] would enable to visualize the structural dynamics starting from the ionized acetylene dimers to the formation of covalently bound $C_4H_4^+$ cations.

ACKNOWLEDGMENTS

This work was jointly supported by the National Natural Science Foundation of China under Grant Nos. 11774281 and 11974272 and the Deutsche Forschungsgemeinschaft (DFG) project. E.W. acknowledges a fellowship from the Alexander von Humboldt Foundation. J.Z. acknowledges support from the China Scholarship Council (CSC).

DATA AVAILABILITY

The data that support the findings of this study are available from the corresponding author upon reasonable request.

REFERENCES

[1] S. A. Sandford, M. Nuevo, P. P. Bera, and T. J. Lee, "Prebiotic astrochemistry and the formation of molecules of astrobiological interest in interstellar clouds and protostellar disks," Chem. Rev. **120**, 4616 (2020).
[2] R. I. Kaiser, "Experimental investigation on the formation of carbon-bearing molecules in the interstellar medium via neutral-neutral reactions," Chem. Rev. **102**, 1309 (2002).
[3] J. Cernicharo, A. M. Heras, A. G. G. M. Tielens, J. R. Pardo, F. Herpin, M. Guélin, and L. B. F. M. Waters, "Infrared space observatory's discovery of C_4H_2, C_6H_2, and benzene in CRL 618," Astrophys. J. **546**, L123 (2001).
[4] T. Y. Brooke, A. T. Tokunaga, H. A. Weaver, J. Crovisier, D. Bockelée-Morvan, and D. Crisp, "Detection of acetylene in the infrared spectrum of comet Hyakutake," Nature **383**, 606 (1996).

[5]P. O. Momoh, A. M. Hamid, S. A. Abrash, and M. Samy El-Shall, "Structure and hydration of the $C_4H_4^{\bullet+}$ ion formed by electron impact ionization of acetylene clusters," J. Chem. Phys. **134**, 204315 (2011).
[6]T. Stein, P. P. Bera, T. J. Lee, and M. Head-Gordon, "Molecular growth upon ionization of van der Waals clusters containing HCCH and HCN is a pathway to prebiotic molecules," Phys. Chem. Chem. Phys. **22**, 20337 (2020).
[7]P. Tarakeshwar, P. R. Buseck, and F. X. Timmes, "On the structure, magnetic properties, and infrared spectra of iron pseudocarbynes in the interstellar medium," Astrophys. J. **879**, 2 (2019).
[8]J. Zhen, T. Chen, and A. G. G. M. Tielens, "Laboratory photochemistry of pyrene clusters: An efficient way to form large PAHs," Astrophys. J. **863**, 128 (2018).
[9]P. P. Bera, R. Peverati, M. Head-Gordon, and T. J. Lee, "Hydrocarbon growth via ion-molecule reactions: Computational studies of the isomers of $C_4H_2^+$, $C_6H_2^+$ and $C_6H_4^+$ and their formation paths from acetylene and its fragments," Phys. Chem. Chem. Phys. **17**, 1859 (2015).
[10]D. S. N. Parker, F. Zhang, Y. S. Kim, R. I. Kaiser, A. Landera, V. V. Kislov, A. M. Mebel, and A. G. G. M. Tielens, "Low temperature formation of naphthalene and its role in the synthesis of PAHs (polycyclic aromatic hydrocarbons) in the interstellar medium," Proc. Natl. Acad. Sci. U. S. A. **109**, 53 (2012).
[11]A. G. G. M. Tielens, "The molecular universe," Rev. Mod. Phys. **85**, 1021 (2013).
[12]E. Herbst and E. F. van Dishoeck, "Complex organic interstellar molecules," Annu. Rev. Astron. Astrophys. **47**, 427 (2009).
[13]P. M. Woods, T. J. Millar, A. A. Zijlstra, and E. Herbst, "The synthesis of benzene in the proto–planetary nebula CRL 618," Astrophys. J. **574**, L167 (2002).
[14]Y. Ono and C. Y. Ng, "A study of the unimolecular decomposition of the $(C_2H_2)_2^+$ complex," J. Chem. Phys. **77**, 2947 (1982).
[15]T. Stein, B. Bandyopadhyay, T. P. Troy, Y. Fang, O. Kostko, M. Ahmed, and M. Head-Gordon, "*Ab initio* dynamics and photoionization mass spectrometry reveal ion–molecule pathways from ionized acetylene clusters to benzene cation," Proc. Natl. Acad. Sci. U. S. A. **114**, E4125 (2017).
[16]R. A. Relph, J. C. Bopp, J. R. Roscioli, and M. A. Johnson, "Structural characterization of $(C_2H_2)_{1-6}^+$ cluster ions by vibrational predissociation spectroscopy," J. Chem. Phys. **131**, 114305 (2009).
[17]B. Bandyopadhyay, T. Stein, Y. Fang, O. Kostko, A. White, M. Head-Gordon, and M. Ahmed, "Probing ionic complexes of ethylene and acetylene with vacuum-ultraviolet radiation," J. Phys. Chem. A **120**, 5053 (2016).
[18]J. S. Knight, C. G. Freeman, M. J. McEwan, V. G. Anicich, and W. T. Huntress, "A flow tube study of ion-molecule reactions of acetylene," J. Phys. Chem. **91**, 3898 (1987).
[19]J. A. Booze and T. Baer, "The photoionization and dissociation dynamics of energy-selected acetylene dimers, trimers, and tetramers," J. Chem. Phys. **98**, 186 (1993).
[20]P. O. Momoh, S. A. Abrash, R. Mabrouki, and M. S. El-Shall, "Polymerization of ionized acetylene clusters into covalent bonded ions: Evidence for the formation of benzene radical cation," J. Am. Chem. Soc. **128**, 12408 (2006).
[21]H. Shinohara, H. Sato, and N. Washida, "Photoionization mass spectroscopic studies of ethylene and acetylene clusters: Intracluster excess energy dissipation," J. Phys. Chem. **94**, 6718 (1990).
[22]M. E. Tuckerman, D. Marx, M. L. Klein, and M. Parrinello, "On the quantum nature of the shared proton in hydrogen bonds," Science **275**, 817 (1997).
[23]Z. Sun, C.-K. Siu, O. P. Balaj, M. Gruber, V. E. Bondybey, and M. K. Beyer, "Proton transfer in ionic water clusters," Angew. Chem., Int. Ed. **45**, 4027 (2006).
[24]E. Wang, X. Shan, L. Chen, T. Pfeifer, X. Chen, X. Ren, and A. Dorn, "Ultrafast proton transfer dynamics on the repulsive potential of the ethanol dication: Roaming-mediated isomerization versus Coulomb explosion," J. Phys. Chem. A **124**, 2785 (2020).
[25]E. Wang, X. Ren, W. Baek, H. Rabus, T. Pfeifer, and A. Dorn, "Water acting as a catalyst for electron-driven molecular break-up of tetrahydrofuran," Nat. Commun. **11**, 2194 (2020).
[26]T. Okino, Y. Furukawa, P. Liu, T. Ichikawa, R. Itakura, K. Hoshina, K. Yamanouchi, and H. Nakano, "Coincidence momentum imaging of ejection of hydrogen molecular ions from methanol in intense laser fields," Chem. Phys. Lett. **419**, 223 (2006).
[27]V. Hrouda, M. Roeselová, and T. Bally, "The $C_4H_4^{\bullet+}$ potential energy surface. 3. The reaction of acetylene with its radical cation," J. Phys. Chem. A **101**, 3925 (1997).
[28]W. Wagner-Redeker, A. J. Illies, P. R. Kemper, and M. T. Bowers, "Structure and reactivity of gas-phase ions: $C_4H_4^{\bullet+}$," J. Am. Chem. Soc. **105**, 5719 (1983).
[29]K. Bartschat and M. J. Kushner, "Electron collisions with atoms, ions, molecules, and surfaces: Fundamental science empowering advances in technology," Proc. Natl. Acad. Sci. U. S. A. **113**, 7026 (2016).
[30]B. C. Garrett, D. A. Dixon, D. M. Camaioni, D. M. Chipman, M. A. Johnson, C. D. Jonah, G. A. Kimmel, J. H. Miller, T. N. Rescigno, P. J. Rossky, S. S. Xantheas, S. D. Colson, A. H. Laufer, D. Ray, P. F. Barbara, D. M. Bartels, K. H. Becker, K. H. Bowen, S. E. Bradforth, I. Carmichael, J. V. Coe, L. R. Corrales, J. P. Cowin, M. Dupuis, K. B. Eisenthal, J. A. Franz, M. S. Gutowski, K. D. Jordan, B. D. Kay, J. A. LaVerne, S. V. Lymar, T. E. Madey, C. W. McCurdy, D. Meisel, S. Mukamel, A. R. Nilsson, T. M. Orlando, N. G. Petrik, S. M. Pimblott, J. R. Rustad, G. K. Schenter, S. J. Singer, A. Tokmakoff, L.-S. Wang, C. Wittig, and T. S. Zwier, "Role of water in electron-initiated processes and radical chemistry: Issues and scientific advances," Chem. Rev. **105**, 355 (2005).
[31]M. A. Huels, B. Boudaïffa, P. Cloutier, D. Hunting, and L. Sanche, J. Am. Chem. Soc. **125**, 4467 (2003).
[32]S. M. Pimblott and J. A. LaVerne, "Production of low-energy electrons by ionizing radiation," Radiat. Phys. Chem. **76**, 1244 (2007).
[33]L. Campbell and M. J. Brunger, "Electron collisions in atmospheres," Int. Rev. Phys. Chem. **35**, 297 (2016).
[34]E. Alizadeh, T. M. Orlando, and L. Sanche, "Biomolecular damage induced by ionizing radiation: The direct and indirect effects of low-energy electrons on DNA," Annu. Rev. Phys. Chem. **66**, 379 (2015).
[35]J. Ullrich, R. Moshammer, A. Dorn, R. Dörner, L. P. H. Schmidt, and H. Schmidt-Böcking, "Recoil-ion and electron momentum spectroscopy: Reaction-microscopes," Rep. Prog. Phys. **66**, 1463 (2003).
[36]X. Ren, T. Pflüger, M. Weyland, W. Y. Baek, H. Rabus, J. Ullrich, and A. Dorn, "An (e, 2e + ion) study of low-energy electron-impact ionization and fragmentation of tetrahydrofuran with high mass and energy resolutions," J. Chem. Phys. **141**, 134314 (2014).
[37]X. Ren, E. Wang, A. D. Skitnevskaya, A. B. Trofimov, K. Gokhberg, and A. Dorn, "Experimental evidence for ultrafast intermolecular relaxation processes in hydrated biomolecules," Nat. Phys. **14**, 1062 (2018).
[38]G. Bieri and L. Åsbrink, "30.4-nm He(II) photoelectron spectra of organic molecules: Part I. Hydrocarbons," J. Electron Spectrosc. Relat. Phenom. **20**, 149 (1980).
[39]M. J. Frisch, G. W. Trucks, H. B. Schlegel, G. E. Scuseria, M. A. Robb, J. R. Cheeseman, G. Scalmani, V. Barone, G. A. Petersson, H. Nakatsuji, X. Li, M. Caricato, A. V. Marenich, J. Bloino, B. G. Janesko, R. Gomperts, B. Mennucci, H. P. Hratchian, J. V. Ortiz, A. F. Izmaylov, J. L. Sonnenberg, D. Williams-Young, F. Ding, F. Lipparini, F. Egidi, J. Goings, B. Peng, A. Petrone, T. Henderson, D. Ranasinghe, V. G. Zakrzewski, J. Gao, N. Rega, G. Zheng, W. Liang, M. Hada, M. Ehara, K. Toyota, R. Fukuda, J. Hasegawa, M. Ishida, T. Nakajima, Y. Honda, O. Kitao, H. Nakai, T. Vreven, K. Throssell, J. A. Montgomery, Jr., J. E. Peralta, F. Ogliaro, M. J. Bearpark, J. J. Heyd, E. N. Brothers, K. N. Kudin, V. N. Staroverov, T. A. Keith, R. Kobayashi, J. Normand, K. Raghavachari, A. P. Rendell, J. C. Burant, S. S. Iyengar, J. Tomasi, M. Cossi, J. M. Millam, M. Klene, C. Adamo, R. Cammi, J. W. Ochterski, R. L. Martin, K. Morokuma, O. Farkas, J. B. Foresman, and D. J. Fox, Gaussian 16, Revision A.03, Gaussian, Inc., Wallingford, CT, 2016.
[40]H. B. Schlegel, J. M. Millam, S. S. Iyengar, G. A. Voth, A. D. Daniels, G. E. Scuseria, and M. J. Frisch, "*Ab initio* molecular dynamics: Propagating the density matrix with Gaussian orbitals," J. Chem. Phys. **114**, 9758 (2001).
[41]S. S. Iyengar, H. B. Schlegel, J. M. Millam, G. A. Voth, G. E. Scuseria, and M. J. Frisch, "*Ab initio* molecular dynamics: Propagating the density matrix with Gaussian orbitals. II. Generalizations based on mass-weighting, idempotency, energy conservation and choice of initial conditions," J. Chem. Phys. **115**, 10291 (2001).
[42]H. B. Schlegel, S. S. Iyengar, X. Li, J. M. Millam, G. A. Voth, G. E. Scuseria, and M. J. Frisch, "*Ab initio* molecular dynamics: Propagating the density matrix with

Gaussian orbitals. III. Comparison with Born–Oppenheimer dynamics," J. Chem. Phys. **117**, 8694 (2002).
[43]P. Plessis and P. Marmet, "Electroionization study of acetylene and fragment ions," Int. J. Mass Spectrom. Ion Processes **70**, 23 (1986).
[44]P. M. Dehmer and J. L. Dehmer, "Observation of bending modes in the $X^2\ \pi_u$ state of the acetylene ion using He(I) photoelectron spectrometry," J. Electron Spectrosc. Relat. Phenom. **28**, 145 (1982).
[45]P. Duffy, S. A. C. Clark, C. E. Brion, M. E. Casida, D. P. Chong, E. R. Davidson, and C. Maxwell, "Electron momentum spectroscopy of the valence orbitals of acetylene: Quantitative comparisons using near Hartree-Fock limit and correlated wavefunctions," Chem. Phys. **165**, 183 (1992).
[46]T. Pflüger, A. Senftleben, X. Ren, A. Dorn, and J. Ullrich, "Observation of multiple scattering in (*e*, 2*e*) experiments on small argon clusters," Phys. Rev. Lett. **107**, 223201 (2011).
[47]S. Karthikeyan, H. M. Lee, and K. S. Kim, "Structure, stabilities, thermodynamic properties, and ir spectra of acetylene clusters $(C_2H_2)_{n=2-5}$," J. Chem. Theory Comput. **6**, 3190 (2010).
[48]S. R. Gadre, S. D. Yeole, and N. Sahu, "Quantum chemical investigations on molecular clusters," Chem. Rev. **114**, 12132 (2014).
[49]A. Karpfen, "The dimer of acetylene and the dimer of diacetylene: A floppy and a very floppy molecule," J. Phys. Chem. A **103**, 11431 (1999).
[50]Z.-H. Loh, G. Doumy, C. Arnold, L. Kjellsson, S. H. Southworth, A. Al Haddad, Y. Kumagai, M.-F. Tu, P. J. Ho, A. M. March, R. D. Schaller, M. S. Bin Mohd Yusof, T. Debnath, M. Simon, R. Welsch, L. Inhester, K. Khalili, K. Nanda, A. I. Krylov, S. Moeller, G. Coslovich, J. Koralek, M. P. Minitti, W. F. Schlotter, J.-E. Rubensson, R. Santra, and L. Young, "Observation of the fastest chemical processes in the radiolysis of water," Science **367**, 179 (2020).
[51]K. Schnorr, A. Senftleben, M. Kurka, A. Rudenko, L. Foucar, G. Schmid, A. Broska, T. Pfeifer, K. Meyer, D. Anielski, R. Boll, D. Rolles, M. Kübel, M. F. Kling, Y. H. Jiang, S. Mondal, T. Tachibana, K. Ueda, T. Marchenko, M. Simon, G. Brenner, R. Treusch, S. Scheit, V. Averbukh, J. Ullrich, C. D. Schröter, and R. Moshammer, "Time-resolved measurement of interatomic coulombic decay in Ne_2," Phys. Rev. Lett. **111**, 093402 (2013).